

Biomolecular papain thin films growth by laser techniques

Enikő György · Jose Santiso · Albert Figueras ·
Gabriel Socol · Ion N. Mihailescu

Received: 22 August 2005 / Accepted: 5 June 2006 / Published online: 5 May 2007
© Springer Science+Business Media, LLC 2007

Abstract Papain thin films were synthesised by matrix assisted and conventional pulsed laser deposition (PLD) techniques. The targets submitted to laser radiation consisted on a frozen composite obtained by dissolving the biomaterials in distilled water. For the deposition of the thin films by conventional PLD pressed biomaterial powder targets were submitted to laser irradiation. An UV KrF* excimer laser source was used in the experiments at 0.5 J/cm² incident fluence value, diminished one order of magnitude as compared to irradiation of inorganic materials. The surface morphology of the obtained thin films was studied by atomic force profilometry and atomic force microscopy. The investigations showed that the growth mode and surface quality of the deposited biomaterial thin films is strongly influenced by the target preparation procedure.

Introduction

Thin films of active biomaterials have a wide range of applications which include pharmaceutical industry [1], proteomics [2, 3], biocompatible coatings [4, 5], or miniaturized biosensors and biochips [6–8]. Techniques as

Langmuir-Blodgett dip coating using self-assembled monolayers [9], photolithography [10], or covalent binding [11] are used currently for biomaterial immobilisation and pattern formation. However, usually these conventional techniques are multi-step procedures of high cost, and in most cases require the presence of toxic chemical substances as well as specific pretreated substrate materials.

Laser radiation is not considered as being useful for processing of structures consisting of biological systems. Due to the high intensity of the pulses, lasers are destructive for active biomaterials. Nevertheless, laser deposition techniques were already tested besides inorganics for organic polymer materials, like polyethylene glycol [12], polyalkylthiophene [13], poly[2-methoxy-5-(2'-ethylhexyloxy)-1,4-phenylene vinylene] [14], various carbohydrates as sucrose, glucose or dextran [15] and also, several biomaterials, as horseradish peroxidase and insulin [16], bovine serum albumine and polyphenol oxidase [17].

One of the major advantages of the laser deposition techniques is that the stoichiometry of the complex multicomponent target molecules can be ensured during their transfer towards the substrate surface [18–20]. Moreover, the amount of material evaporated and deposited on the substrate surface can be easily controlled by the number and/or intensity of the laser pulses used for the irradiation of the targets. In addition, practically any kind of substrate materials can be used, without any pre-treatment procedure.

The purpose of our work is to elucidate how the target preparation procedures, i.e. biomaterial concentration in the frozen composite, or conventional powder pressing influence the thin films growth mode and surface morphology, and to identify the optimum

E. György (✉) · G. Socol · I. N. Mihailescu
National Institute for Lasers, Plasma and Radiations Physics,
P.O. Box MG 36, Bucharest V 76900, Romania
e-mail: eniko@ifin.nipne.ro

E. György · J. Santiso · A. Figueras
Consejo Superior de Investigaciones Científicas, Instituto de
Ciencia de Materiales de Barcelona, Campus UAB, Bellaterra
08193, Spain

conditions which lead to the deposition of uniform and continuous thin films. We focused our attention on papain, a protein-cleaving enzyme derived from papaya plant. The functions of papain are well known, being employed to treat ulcers, reduces fever after surgery, is active against gram-positive and gram-negative bacteria, and has beneficial effects in systemic enzyme therapy in oncology [21].

Experimental

The thin film depositions were performed inside a stainless steel irradiation chamber. A pulsed UV KrF* ($\lambda = 248$ nm, $\tau_{\text{FWHM}} \approx 20$ ns) excimer laser source was used for the targets' irradiation. The composite targets were prepared by dissolving papain in distilled water. The obtained solutions of 1 or 2 wt.% of papain were frozen in liquid nitrogen. For the growth of the reference thin films by conventional PLD the targets were prepared from powders of papain by pressing at 3 MPa.

The laser beam was focused onto the target surface with a 30 cm FD MgF₂ lens placed outside the irradiation chamber. To avoid significant changes in the surface morphology of the targets they were rotated during the multipulse laser irradiation with a frequency of 3 Hz. The angle between the laser beam and the target surface was chosen of 45°. For the deposition of each film we applied 10⁴ subsequent laser pulses, succeeding each other with a repetition rate of 2 Hz. The laser fluence on the target surface was about 0.5 J/cm².

The irradiation chamber was evacuated down to a residual pressure of 10⁻⁵ Pa. The residual gases were monitored with an Amatek MA 100 quadrupole mass spectrometer. All deposition experiments were performed in vacuum.

The n type (111) Si substrates were placed parallel to the target at a separation distance of 3 cm. Prior to introduction inside the deposition enclosure the substrates were carefully cleaned in ultrasonic bath in acetone. During the irradiation the substrates were kept at room temperature, while the frozen targets were cooled, circulating liquid nitrogen inside the rotating target holder.

The surface morphology and growth mode of the deposited papain thin films were investigated by atomic force microscopy in acoustic (dynamic) configuration with a PicoSPM Molecular Imaging apparatus. From the obtained data the porosity of the surface and the volume of deposited material were evaluated with the aid of the MountainsMap computer simulation program from Digital Surf. The thickness of the thin films was measured by a KLA Tencor Nanopics 2100 atomic force profilometer.

Results and discussion

Figure 1 shows the AFM images of thin films obtained in the same experimental conditions, but from targets containing different papain concentration. At the lower, 1 wt.% papain concentration (Fig. 1a) the deposited material forms clusters, with diameters from a few tens to a few hundreds of nanometers. As can be observed in the image, the small, tens of nanometer diameter clusters are separated or constitute groups of islands rather than a continuous layer. In case of the target containing higher, 2 wt.% papain (Fig. 1b), the deposition has similar surface morphology, characterized by cluster formation. Nevertheless, the clusters density is much higher, covering the substrate surface, in form of a continuous thin film.

In Fig. 2a,b we present in detail the surface of this deposition. The clusters' diameters have a quite narrow

Fig. 1 AFM images of the thin films obtained by the irradiation of the (a) 1 and (b) 2 wt.% concentration frozen composite targets

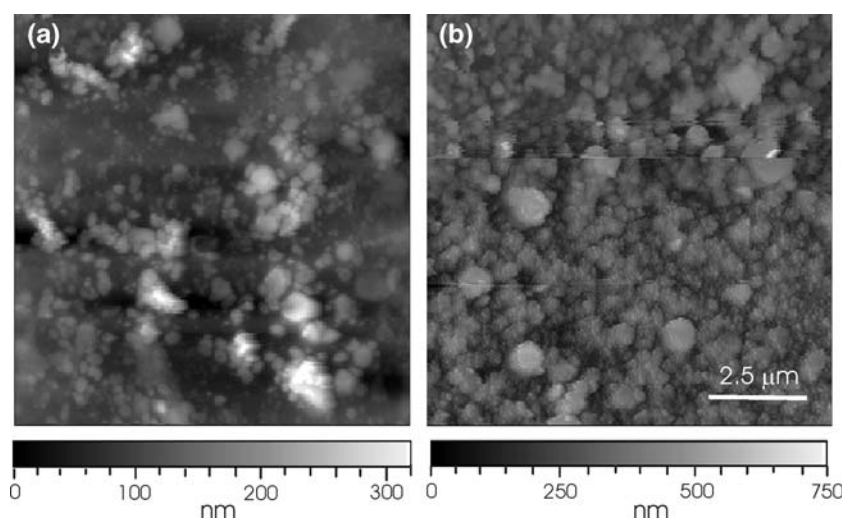
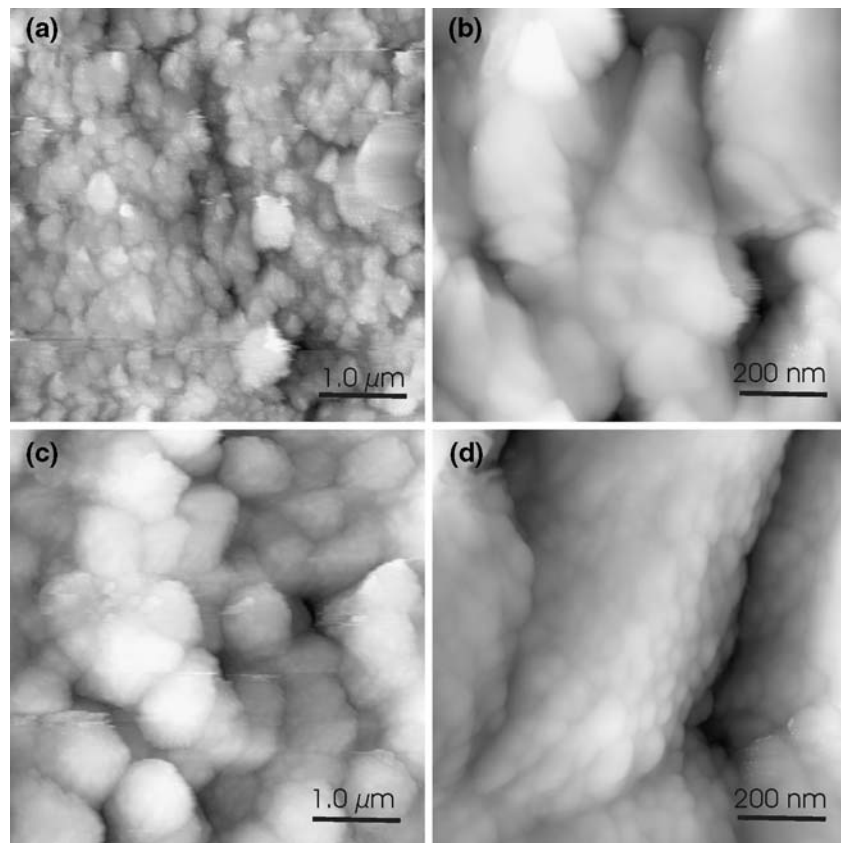


Fig. 2 AFM images of the thin films obtained by the irradiation of the (a, b) 2 wt.% concentration frozen composite and (c, d) pressed power targets



range of distribution, with an average value around 200 nm. Nevertheless, from the higher magnification image (Fig. 2b) one can observe that the clusters are conglomerates formed by smaller, tens of nanometers diameter nanoparticles. As a next step, we compared the surface morphology of the depositions obtained from the frozen composite targets with that obtained by the irradiation of a pressed powder target of papain (Fig. 2c,d). This last deposition is composed by much larger grains, with diameters in the micrometer range. Moreover, as can be observed in the higher magnification image, the grains are covered by dense, closely packed nanoparticles with very similar shapes and dimensions, in the range of tens of nanometers.

The surface profiles of the depositions obtained from the three different targets are presented in Fig. 3. The profile of the deposition obtained from the 1 wt.% target is rather smooth, reproducing the shape of the isolated nanoparticles (curve a). Conversely, in curve b corresponding to the deposition from the 2 wt.% target the irregular shape of the surface profile proves the formation of larger clusters constituted by nanoparticles. The profile of the deposition obtained from the pressed powder target (curve c) is completely different, shows a large surface roughness, due to the large grains, with dimensions in the micrometer

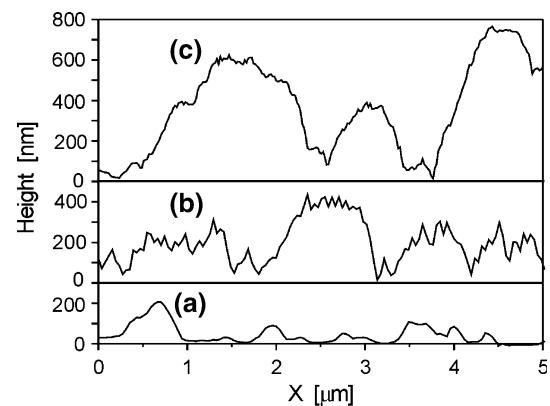


Fig. 3 Surface profiles of thin films obtained by the irradiation of the (a) 1 and (b) 2 wt.% concentration frozen composite, as well as (c) pressed power targets

range (curve c). The same trend can be observed in the histograms of local heights of the depositions (Fig. 4). Moreover, the increase of the histograms area indicates the increase of the particles density on the substrate surfaces.

The minimum root-mean square (r.m.s.) surface roughness of the deposited materials was calculated from the AFM data. The surface roughness increases from about 30 nm for the deposition obtained from the 1 wt.% to about

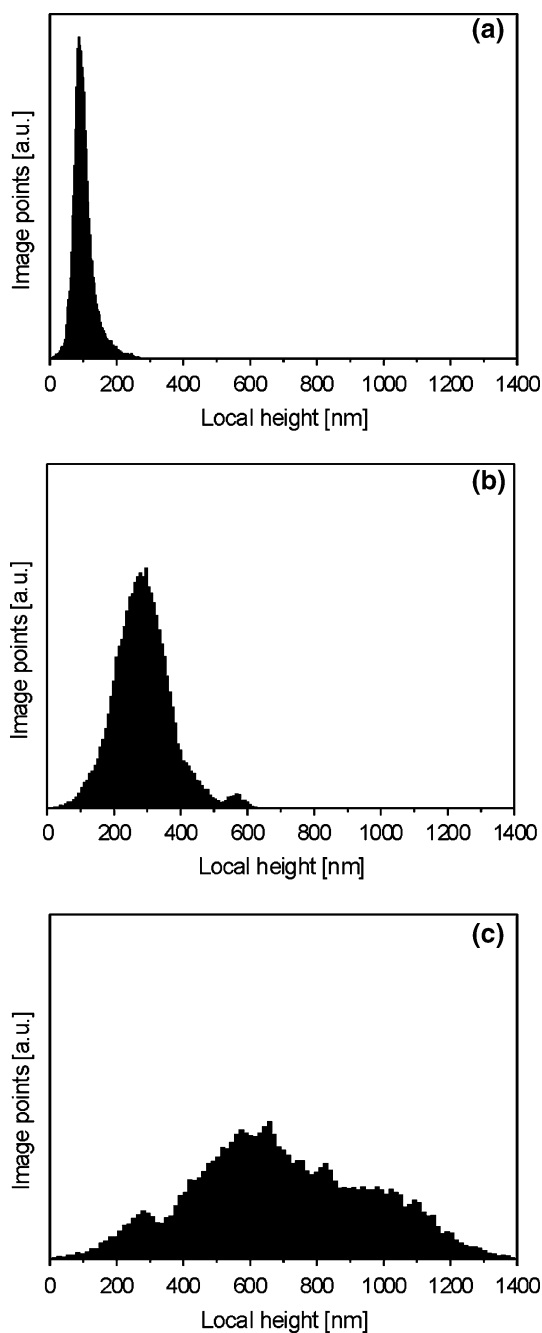


Fig. 4 Histograms of local heights counted on $10 \times 10 \mu\text{m}^2$ surface areas of thin films obtained by the irradiation of the (a) 1 and (b) 2 wt.% concentration frozen composite, as well as (c) pressed power targets

70 nm for the deposition obtained from the 2 wt.% composite. We recall that tens of nanometers roughness values when using frozen composite targets are characteristic for organic material deposition [22]. Similar, or even higher roughness values were reported also for biomaterial, insulin and horseradish peroxidase, thin films [16]. As compared to the depositions from composite targets, the

roughness of the film obtained from the pressed powder target is very large, about 250 nm.

In Fig. 5 we represented the accumulated surface porosity (A) as well as volume (B) of the depositions obtained from the 1 (curves a) and 2 wt.% (curves b), as well as pressed powder (curves c) targets as a function of heights measured from the substrate surface. Thus, the last values at the maximum heights correspond in each case to the total porosity percentage as well as total deposited volume. In case of the 1 wt.% target it can be seen the absence of a continuous thin film on the substrate. Conversely, at 2 wt.% concentration there exists a compact thin film with a thickness value of about 180 nm, followed by a layer until the maximum height of about 600 nm, denser as compared to the deposition obtained from the 1 wt.% target. The porosity value of the films obtained from the pressed powder target at the maximum height (about 1300 nm) is similar to that corresponding to the deposition obtained from the 2 wt. % target.

The thickness value measured by atomic force profilometry for the film deposited from the 1 wt.% target is similar with the average local heights evaluated from the

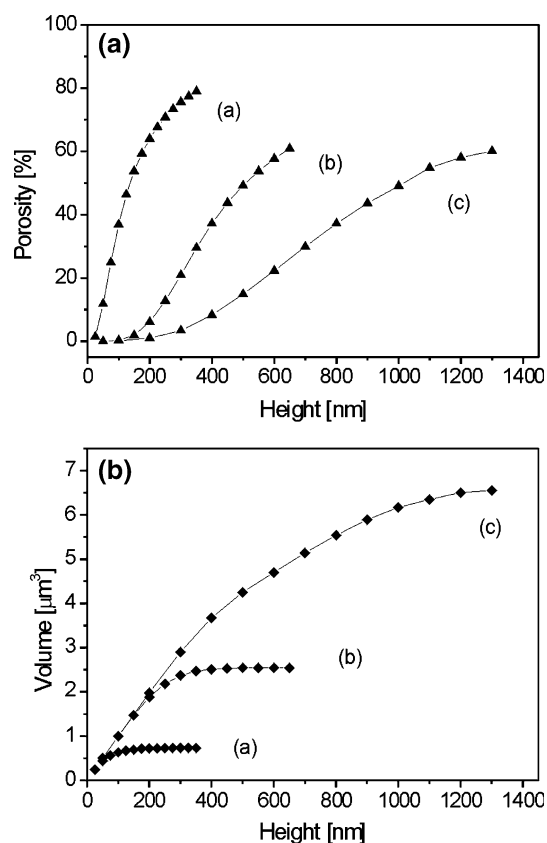


Fig. 5 (A) Surface porosity and (B) volume measured on $10 \times 10 \mu\text{m}^2$ surface areas of thin films obtained by the irradiation of the (a) 1 and (b) 2 wt. % concentration frozen composite, as well as (c) pressed power targets

Table 1 Thin films thickness, z, r.m.s. surface roughness, clusters mean diameter, d, average local height, h, surface porosity [%], and total deposited volume, V, on $10 \times 10 \mu\text{m}^2$ substrate surface areas as a function of the target preparation conditions

Target	z [nm]	r.m.s. [nm]	d [nm]	h [nm]	Porosity [%]	V [μm^3]
1 wt.% composite	90	30	100	90	80	0.7
2 wt.% composite	420	70	200	240	60	2.5
Pressed powder	1000	250	800	700	60	6.5

AFM image. In case of the films deposited from the 2 wt.% and pressed powder targets the difference between the thickness values and average local heights, confirms the existence of a compact thin layer in the vicinity of the substrate surface.

We present in Table 1 a summary concerning the thickness, r.m.s. surface roughness, clusters mean diameter, average local height, surface porosity, and total volume of the deposited material on $10 \times 10 \mu\text{m}^2$ substrate surface area, as a function of the target preparation conditions. The completely different surface features as regards amount of deposited material, particles morphology and dimensions could be attributed to the laser-material interaction and ablation processes taking place in case of the frozen composite as well as pressed powder targets. Indeed, the large, micrometer sized particulates observed in case of the thin film obtained from the pressed powder target could originate directly from the irradiated target surface, while the tens of nanometers dimensions nanoparticles could form by clusterisation mechanisms taking place during the transit of the ablated material from the target towards the substrate, or on the substrate surface [18–20].

Conclusions

Papain thin films were grown by matrix assisted and conventional pulsed laser deposition techniques. The effect of the target characteristics, as biomaterial concentration in the frozen composites, or conventional powder pressing, on the deposited films growth mode and surface morphology was investigated by atomic force profilometry and atomic force microscopy. Our results indicate that there exist the possibility to control by means of the target preparation procedure the amount of the deposited material and its surface morphology. We succeeded to identify the optimum target preparation conditions, frozen composites from 2 wt.% papain solvent, which lead to the deposition of

uniform continuous thin films, with surface roughness of a few tens of nanometers.

Acknowledgements Financial support from NATO under the contract EAP.RIG 981200 and Romanian Ministry for Education and Research under the contract 150/2006 CEEX is acknowledged with thanks.

References

1. M. A. COOPER, *Nat. Rev. Drug Discov.* **1** (2002) 515
2. P. WAGNER and R. KIM, *Current Drug Discov.* **5** (2002) 23
3. H. MIYACHI, A. HIRATSUKA, K. IKWBUKURO, K. YANO, H. MUGURUMA and I. KARUBE, *Biotechnol. Bioeng.* **69** (2000) 323
4. S. BORMAN, *Chem. Eng. News* **78** (2000) 31
5. M. GERRISTSEN, A. KROS, V. SPARAKEL, J. A. LUTTERMAN, R. J. M. NOLTE and J. A. JANSEN, *Biomaterials* **21** (2000) 71
6. S. A. BROOKS, N. DONTA, C. B. DAVIS, J. K. STUART, G. O'NEILL and W. G. KUHR, *Anal. Chem.* **72** (2000) 3253
7. S. J. DONG and B. Q. WANG, *Electroanalysis* **14** (2002) 7
8. B. KASEMO, *Surf Sci.* **500** (2002) 656
9. I. FUJIWARA, M. OHNISHI and J. SETO, *Langmuir* **8** (1992) 2219
10. C. S. LEE, S. H. LEE, S. S. PARK, Y. K. KIM and B. G. KIM, *Biosens. Bioelectron.* **18** (2003) 437
11. R. A. WILLIAMS and H. W. BLANCH, *Biosens Bioelectron.* **9** (1994) 159
12. D. M. BUBB, P. K. WU, J. S. HORWITZ, J. H. CALLAHAN, M. GALICIA, A. VERTES, R. A. MCGILL, E. J. HOUSER, B. R. RINGEISEN and D. B. CHRISSEY, *J. Appl. Phys.* **91** (2002) 2055
13. A. GUTIERREZ-LLORENTE, G. HORWITZ, R. PEREZ-CASERO, J. PERRIERE, J. L. FAVE, A. YASSAR and C. SANT, *Org. Electron.* **5** (2004) 29
14. B. TOFTMANN, M. R. PAPANTONAKIS, R. C. Y. AU-YEUNG, W. KIM, S. M. O'MALLEY, D. M. BUBB, J. S. HORWITZ, J. SCHOU, P. M. JOHNSEN and R. F. HAGLUND, *Thin Solid Films* **453–454** (2004) 177
15. A. PIQUÉ, D. B. CHRISSEY, B. J. SPARGO, M. A. BUCARO, R. W. VACHET, J. H. CALLAHAN, R. A. MCGILL, D. LEONHARDT and T. MLSNA, *Mater. Res. Soc. Symp. Proc.* **526** (1998) 421
16. B. R. RINGEISEN, J. CALLAHAN, P. K. WU, A. PIQUE, B. SPARGO, R. A. MCGILL, M. BUCARO, D. M. BUBB and D. B. CHRISSEY, *Langmuir* **17** (2001) 3472
17. P. K. WU, B. R. RINGEISEN, D. B. KTIZMAN, C. G. FRONDOZA, M. BROOKS, D. M. BUBB, R. C. Y. AU-YEUNG, A. PIQUÉ, B. SPARGO and R. A. MCGILL, *Rev. Sci. Instrum.* **74** (2003) 2546
18. L. C. CHEN, *Pulsed Laser Deposition of Thin Films*, edited by D. G. CHRISSEY and G. K. HUBLER (Wiley: New York, 1994) p. 167
19. D. BÄUERLE, *Laser Processing and Chemistry* (Springer: Berlin, 1996) p. 63
20. I. N. MIHAILESCU and E. GYÖRGY, *Trends in Optics and Photonics* edited by T. ASAKURA (Springer: Berlin, 1999) p. 201
21. J. LEIPNER and R. SALLER, *Drugs* **59** (2000) 769
22. A. PIQUÉ, R. C. Y. AU-YEUNG, J. L. STEPNOWSKI, D. W. WEIR, C. B. ARNOLD, R. A. MCGILL and D. B. CHRISSEY, *Surf. Coat. Technol.* **163–164** (2003) 293